Published by IOP Publishing for Sissa Medialab

Received: *September 16, 2019*
Revised: *November 27, 2019*
Accepted: *January 29, 2020*
Published: *March 3, 2020*

TECHNICAL REPORT

Scintillation detector fault diagnosis based on wavelet packet analysis and multi-classification support vector machine

Y.X. Xie,[a,b] **Y.J. Yan,**[a,1] **G.F. Li**[c] **and X. Li**[a]

[a] *College of Nuclear Science and Technology, University of South China, Hengyang, Hunan Province 421001, China*
[b] *College of Physics and Electronic Engineering, Hengyang Normal University, Hengyang, Hunan Province 421008, China*
[c] *Ling Ao Nuclear Power Co., Ltd., Shenzhen, Guangdong Province 518000, China*

E-mail: 515885997@qq.com

Abstract: This paper presents a scintillation detector fault diagnosis method based on wavelet packet analysis and multi-classification support vector machine(multi-SVM). In the proposed method, a wavelet packet algorithm is used to analyze waveform characteristics of output signals caused by different faults of detectors, then characteristic vectors can be extracted. The multi-SVM is employed to establish a fault recognition model and fault types can be concluded. Performances of the proposed method are validated by experimental data obtained from the plastic scintillation detector for the single fault diagnosis and hybrid fault diagnosis. The experimental results show that faults can be diagnosed automatically and quickly by analyzing signal waveform features.

Keywords: Analysis and statistical methods; Models and simulations; Radiation monitoring; Gamma detectors (scintillators, CZT, HPGe, HgI etc)

[1]Corresponding author.

https://doi.org/10.1088/1748-0221/15/03/T03001

2020 JINST 15 T03001

Contents

2020 JINST 15 T03001

1 Introduction

Various nuclear detectors, which are essential sources of nuclear radiation information and important devices for radioactive monitoring of nuclear facilities, are commonly used to measure intensities of radiations in a nuclear power plant [1]. As ones of them, scintillation detectors are important and widely used in detecting of particles. Their reliabilities have critical impacts on the safety of radiation sites [2]. However, bad conditions, such as intense radiation damages, high temperatures and strong humidities, will accelerate aging probes and result in frequent instrument failures [3]. As always, manual troubleshootings are cumbersome and time-consuming, and followed misjudgements may cause radiation accidents. Consequently, it is necessary to explore an efficient and stable fault diagnosis method which monitors operating data of scintillation detectors and attempts to locate faults in time, then immediate measurements to prevent the system from catastrophic accidents would follow.

Fault diagnosis can improve maintenance efficiency and reduce maintenance costs [4]. Currently, numerous achievements have been obtained regarding the fault diagnosis of nuclear power industries, especially nuclear power plants [5].Reference [5] propose an online diagnostic method based on model-based for faults. Faults in the system are detected and diagnosed by checking consistency between the observed behavior and the predicted behavior through the model. However, practical applications of model-based methods are very limited due to the requirement of an accurate model that is always hard to obtain in practice. In reference [6], a data-driven method for faults is proposed. The empirical model is used to estimate true values of new measurements, and faults are detected and diagnosed by evaluating the estimation residuals. In reference [7], signal-based methods make decisions by comparing features(e.g., spectrum) extracted from a signal of desired normal baseline values. Reference [8] reports on the application of Principal Component analysis

(PCA) for pulse-shape discrimination (PSD) of scintillation radiation detectors. It depicts great advantages of automatic extraction of the pulse-shape characteristics of PCA analysis. However, PCA cannot identify the classification of the samples and expands the difference among all samples.

In this paper, a fault diagnosis model is proposed for scintillation detectors based on wavelet packet analysis and multi-classification support vector machine (multi-SVM). With great advantages of decomposing and reconstructing signals, of performing the multilevel frequency division of the whole band, of displaying signal characteristics at different levels, the wavelet packet analysis based on wavelet transform has wide applications in analog circuits, sensors, mechanical fault diagnosis and signal noise reduction [9]. The multi-SVM, which is based on machine learning, is an excellent classifier of the fault diagnosis of systems and equipments [10]. Deriving from a mathematical model in scintillation detectors, there are four types of faults: scintillator aging fault, photomultiplier fault, resistor and capacitor (RC) circuit fault, and radiation damage fault. By using wavelet packet algorithm, current signals of faults could be decomposed and analyzed. Energy characteristic vectors were calculated by using wavelet decomposition coefficients, which can tell the different changes of waveform characteristics of output signals [11]. A multi-SVM diagnosis model is established by recognizing the four types of scintillation detectors faults through the energy vectors. This model is practical in engineering application in proof of the training of history data and the recognition of monitoring data.The validity of this model is verified through simulations.

2 Methods

As a result of complexities and diversities of scintillation detector faults, traditional classification methods can bare determine the existence of a fault. However, these methods can not accurately locate faults and catalog the types. In this study, a mathematical model, which is based on wavelet packet analysis and multi-SVM method, is proposed to detect and classify various faults of scintillation detectors.

2.1 Modelling for normal and fault detector output signals

The plastic scintillation detector signal is a series of random pulse signals with specific shapes. Time interval of adjacent pulses abides by the rule of exponential distribution, the output pulse amplitude and noise followed the Gaussian distribution have statistical characteristics, and the output pulse waveform can be approximately expressed by the double exponential function. Equation (2.1) shows the function representation:

$$v_0(t) = u(t) \cdot A(e^{-t/\tau_1} - e^{-t/\tau_2}) + v(t), \tag{2.1}$$

where $u(t)$ indicates the step function; A is the signal amplitude; v(t) is the white noise superimposed on the signal; τ_1 and τ_2 are the fast and slow time constants of the double exponential function respectively, both of which determined the decay time jointly. By using equation (2.1) to set the three parameters of signal amplitude, white noise and decay time, the mathematical model of four types of faults which are scintillator aging, photomultiplier, RC circuit and radiation damage faults is established.

The scintillation detector ages with operatings under high-temperature surroundings for a long time. Moreover, the luminous efficiency of scintillator gradually decreases, and the output of light

2020 JINST 15 T03001

gradually reduces. In this model, 20% reduction of light outputs is catalogued as the aging fault, which manifests changes on the pulse height and corresponds to A in equation (2.1). For providing sufficient samples in the multi-SVM, this experiment simulates 100 sets of fault signals from the range 35% to 80% of the original efficiency.

The photomultiplier tube is an electric vacuum. Its performances, such as sealing capability, amplification ability, and current noises, deteriorated as situations like external force impact, the photomultiplier tube seat or pins are damp or stained and the strong-radiation field. Specially, its noise caused by dark currents increases dramatically. Citing an no-exceeding 10 times of dark currents instance in the study, the photomultiplier fault is defined as noises exceeding the deadline of that under normal working. Furthermore, in this model, the range of 10 to 15 times of an increase of noise is catalogued as the photomultiplier fault, which manifests changes on the noise increase and corresponds to v(t) in equation (2.1). This experiment simulates 100 groups of fault signal waveform data.

The scintillation detector analogy output circuit can be equivalent to an output circuit consisting of an RC and a preamplifier. The detector converts the incident particle energy into a charge number, forms a current pulse, and outputs a voltage pulse through the RC loop impedance. In this method, 50% changes of the component values in R or C are considered to be a soft fault model [12]; That is, a RC fault is defined in following three cases like RC value exceeding or equal 4 times, RC value shrinking by 3/4 or more, RC value tending to infinity. This experiment simulates a 100-group RC value including all three cases which can be set through τ_1 and τ_2 in equation (2.1).

In addition, there are two aspects of changes of a scintillation detector after a long term under radiation: an increasing of noise output and a decreasing of light output. Under normal circumstances, a probe cannot meet the radiation resistance requirement if a 15% reduction luminous efficiency of the scintillator. Consequently, the radiation damage fault is characterized by two conditions: a reduction from the range 35% to 85% of the original luminous efficiency and an increasing of more than 10 times of noise outputs. The former one could be set through A in equation (2.1), the other through V(t) either. This study simulates 100 sets of fault signal waveform data.

According to the variation characteristics of output signal waveforms caused by the typical four types of faults described above, the pulse amplitude of the signal, the energy resolution, the white noise standard deviation, the expectation, and the fast and slow time constants are equal to 1 V, 15%, 0.005, 0, 5, and 30, respectively [13]. Comparisons of the various faults shown in figure 1 with one normal nuclear signal in one single pulse are simulated. Among them, the aging fault reflects a signal waveform where the luminous efficiency drops 50%. The photomultiplier fault reflects an another waveform where noises are 10 times higher than the usual. The RC fault (a) presents the value of RC has quadrupled, RC fault (b) presents it has shrunk by 3/4, and RC fault (c) presents it tends to infinity. Furthermore, the radiation damage fault reflects one signal waveform in both cases where the luminous efficiency became 55% and the noise doubled 5 times.

2.2 Extracting characteristic vectors by wavelet packet analysis

The detector output signal is decomposed into approximate and detail coefficients by the wavelet packet algorithm which extract the eigenvectors of nuclear signals. Different wavelet basis functions induce different results, even for identical output signals. In order to determine one suitable function,

2020 JINST 15 T03001

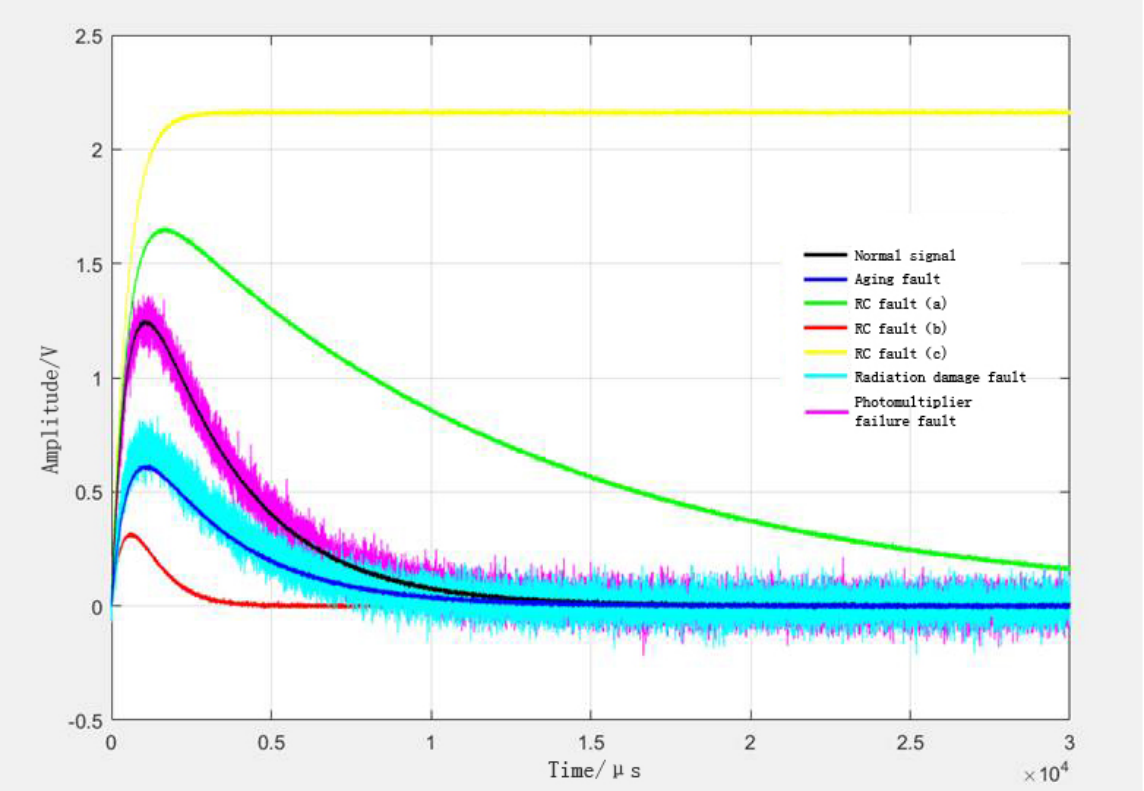

Figure 1. Comparisons of various faults signals with one normal nuclear signal.

some important rules must be obeyed, such as the self-similarity principle, the discriminant function and the support length. Therefore, the db4 wavelet basis function combined with characteristics of detector output signals is fully qualified for the high regularity with comprehensive considerations of the relationship between support length and vanishing moment. This function performs a three-layer decomposition of random nuclear signals of nodes which gives coefficients of different frequency bands sequently, then energies of nodes are calculated as characteristic vectors. As a fault occurs, energies of each node change, the fault signal can be distinguished from normal one. Consequently, the selected has not only the compact support feature, also good time-frequency characteristics.

The wavelet packet algorithm decomposes the output signal of scintillation detectors, and steps for signal characteristic extraction are as follows [9]:

(a) The detector output signal x is normalized:

$$x' = D_{\sigma}^{-1} \left[x - E\left(X\right) \right], \tag{2.2}$$

where x represents the detector output signal sequence; $E\left(X\right)$ is the expectation of x; and D_{σ} is the standard deviation of x.

(b) The three-layer wavelet packet decomposition is performed on x', and the decomposition coefficient vectors of the eight different frequency bands of the third layer from low to high are respectively represented by x'_{30}, x'_{31}, x'_{32}, x'_{33}, x'_{34}, x'_{35}, x'_{36}, x'_{37}.

2020 JINST 15 T03001

(c) Total energy$E_{S_{3i}}$ of each frequency band signal is calculated according to equation (2.3):

$$E_{S_{3i}} = \int |x_{3i}|^2 \, dt = \sum_{j=1}^{n} \left| x_{3i,j} \right|^2 , \tag{2.3}$$

where n is the number of decomposition coefficients in each band.

(d) Normalize to $E_{S_{3i}}$, and a characteristic vector T is constructed.

$$\overline{E_{S_{3i}}} = \frac{E_{S_{3i}}}{\sum_{i=0}^{7} E_{S_{3i}}}, \tag{2.4}$$

$$T = \left[\overline{E_{S_{30}}}, \overline{E_{S_{31}}}, \overline{E_{S_{32}}}, \overline{E_{S_{33}}}, \overline{E_{S_{34}}}, \overline{E_{S_{35}}}, \overline{E_{S_{36}}}, \overline{E_{S_{37}}} \right] , \tag{2.5}$$

Table 1 gives the set of characteristic vectors obtained by the wavelet packet algorithm before and after faults happened in cases shown in figure 1.

Table 1. Normalized table of eigenvectors.

Detector state	$\overline{E_{S_{30}}}$	$\overline{E_{S_{31}}}$	$\overline{E_{S_{32}}}$	$\overline{E_{S_{33}}}$	$\overline{E_{S_{34}}}$	$\overline{E_{S_{35}}}$	$\overline{E_{S_{36}}}$	$\overline{E_{S_{37}}}$
Normal	0.99990	0.00511	0.00510	0.00504	0.00502	0.00506	0.00506	0.00513
Aging fault	0.99977	0.00804	0.00820	0.00819	0.00800	0.00797	0.00812	0.00797
Photomultiplier fault	0.98883	0.05605	0.05555	0.05510	0.05657	0.05628	0.05755	0.05709
RC fault (a)	0.99998	0.00220	0.00218	0.00223	0.00222	0.00214	0.00221	0.00219
RC fault (b)	0.99706	0.02883	0.02893	0.02916	0.02921	0.02867	0.02853	0.02929
RC fault (c)	0.99999	0.00087	0.00087	0.00086	0.00088	0.00089	0.00088	0.00086
Radiation damage fault	0.96724	0.09574	0.09561	0.09613	0.09773	0.09636	0.09362	0.09632

Table 1 shows that the energy of detector signals does not change apparently in the first column (the first low frequency band) with the comparation between normal conditions and faulty conditions. However, the energy changes in the high-frequency band are more pronounced because of most of the energy concentrating at the first low-frequency band.

2.3 Fault diagnosis based on multi-classification support vector machine

Multi-classification support vector machine (multi-SVM) is a machine-learning algorithm based on statistical learning machine theory [14]. Innovations of the theory are saving spaces and computational complexity in practical applications for the machine-learning with small samples. The basic principle of the theory is structural risk minimization. It can ensure that the number of training samples is small enough, and the training ability is optimized, which speeds up the operation and makes up for disadvantages of the traditional learning machine such as large computations, slow convergence and large data samples. According to the principle of that theory, the multi-SVM method seeks the best compromise between the model complexity and the learning ability based on limited sample information to obtain the best generalization ability, thereby facilitating the quick and accurate classification and locating faults in nuclear detectors [15]. It is very suitable for classifying nuclear random signals.

2020 JINST 15 T03001

For separable samples: $(x_i, y_i), i = 1, 2, \cdots, N, x_i \in R^n, y_i \in \{-1, +1\}$, an optimal separating hyperplane H: $\omega \cdot x + b = 0$ can accurately divide the samples into two categories. The support vectors are defined as two types of sample vectors nearest to the hyperplane. Meanwhile, the summation of distance between the two types of support vectors and hyperplane is $2/\|\omega\|$. ω is a normal vector of hyperplane H. The classification problem is creating an optimal hyperplane which can be transformed to an optimization problem [16]:

$$y_i\left((\omega \cdot x_i) + b\right) \geq 1, i = 1, 2, \cdots, N; \underbrace{\min}_{\omega, b} \frac{1}{2}\|\omega\|^2 \tag{2.6}$$

where b is the threshold. The constraint condition shows the distance between each sample and the optimal hyperplane H is greater than or equal to 1. However, data samples in the training dataset are linearly inseparable for most application cases.

Therefore, a slack variable ξ_i is substituted into multi-SVM and a penalty parameter C is added to minimize ξ_i. Thus, the objective function can be changed to

$$y_i\left((\omega \cdot x_i) + b\right) \geq 1 - \xi_i, i = 1, 2, \cdots, N; \underbrace{\min}_{\omega, b} \frac{1}{2}\|\omega\|^2 + C\sum_{i=1}^{N}\xi_i \tag{2.7}$$

This problem can be solved using the Lagrange multiplier method. The corresponding constraint condition is $\sum_{i=1}^{N}\alpha_i y_i = 0, \alpha_i \geq 0$, where α_i is the Lagrange multiplier. For nonlinear cases, ϕ(x) can be applied to map samples in the low-dimensional space to the high-dimensional space, where samples can be separated linearly in the high-dimensional space. Define the kernel function $K(x_i, x_j) = \phi(x_i)^T\phi(x_j)$, the optimized objective function can be expressed as:

$$L = \sum_{i=1}^{N}\alpha_i - \frac{1}{2}\sum_{i,j=1}^{N}\alpha_i\alpha_j y_i y_j K\left(x_i, x_j\right) \tag{2.8}$$

Usually, the Gaussian kernel function is chosen as the kernel one. Main advantage of this function is that it can map the samples to higher dimensional spaces. Compared with other kernel functions, it needs less parameter than others, these parameters effectively reduce the computational complexity of numerical values. There is a fact: plastic scintillation detectors have fewer fault characteristics and moderate sample sizes. The chosen function is more suitable for classifying fault signals according to the fact. Penalty parameter C and kernel parameter $\gamma(\gamma = 1/(2 \cdot \sigma 2))$, are important factors that significantly influence the performance of multi-SVM. They must be optimized in advance.

$$K\left(x_i, x_j\right) = \exp\left[-\frac{\left\|x_i - x_j\right\|^2}{2\sigma^2}\right] \tag{2.9}$$

2.4 Multi-SVM -based classification strategy

Multi-SVM is an essentially binary classifier [17].In the case of single fault diagnosis, the multi-SVM establishes only one classifier. In another case of dealing with multifaults, the number of classifiers must be equal to that of fault modes minus one. To improve its applicability, several methods have been suggested for extending multi-SVM, including one-versus-one (1-v-1) and one-versus-rest (1-v-r) [18, 19]. In this research, multi-SVM using 1-v-r SVM strategy is designed

2020 JINST 15 T03001

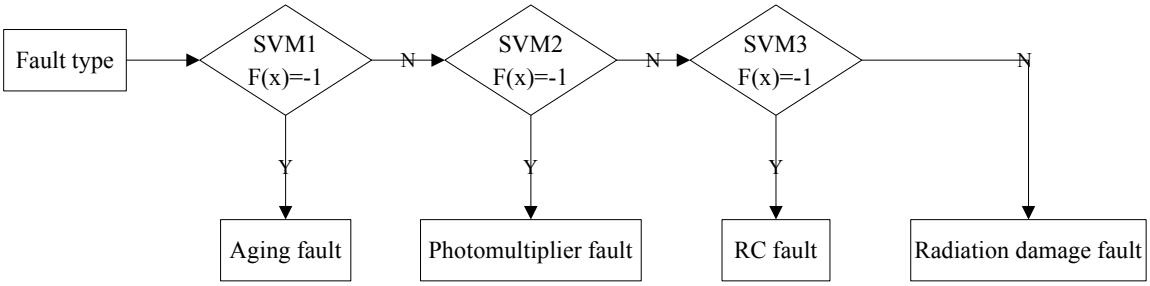

Figure 2. Multi-SVM-based classification strategy.

to realize hybrid fault diagnosis for a plastic scintillation detector (shown in figure 2). Greater values indicate a further distance between input samples and the classification hyperplane, and classification results are more reliable. There are four fault types to be classified: scintillator aging fault, photomultiplier fault, RC fault and radiation damage fault.

SVM1 is trained to separate the scintillator aging fault from the other three fault types. As an input is characterized as the aging fault, a correlated output of SVM1 is set to -1 then the classification process ends; Otherwise, the output is set to $+1$, the process continues and transfers the output to SVM2.

SVM2 is trained to classify the photomultiplier fault from the rest three types. Taken the transferred output as a new input, SVM2 determines an output to be -1 and the process ceases if the input owns the feature of photomultiplier fault, or the output is set to $+1$, and the process keeps moving forward.

SVM3 is for classifying RC fault and radiation damage fault. Continued with previous step, SVM3 assorts faults into two kinds due to their features, two values are given as $+1$ and -1, -1 indicates the RC fault type and $+1$ indicates the rest one, then the process quits.

2.5 Fault diagnosis mechanism

Wavelet packet analysis determines characteristics of scintillation detectors' faults and constructs energy vectors. Wavelet transform is capable for time-frequency analysis and suitable for non-stationary fault signals, then multi-SVM gives a diagnosis model to solve the contradiction between the learning ability and the generalization ability of machine learning. Excellent learning and classification accuracy can be achieved, especially for small sample problems. The fault diagnosis mechanism is shown in figure 3. The key steps are described as follows:

Step 1: The db4 wavelet basis function is applied for performing three-layer analysis of fault signals. A specific process follows equations (2.2) to (2.5) for obtaining one energy vector which reflects fault characteristics.

Step 2: All vectors gather around and construct a database according to step 1. These vectors are then used to train a model from Multi-SVM.

Step 3: The after-training model gives a detail classification at a new fault signal's arrival on one hand; an energy vector of the new signal is extracted by the function in step 1, calculated and saved to the database for further training on the other hand. This process would start over and over while a new signal comes.

2020 JINST 15 T03001

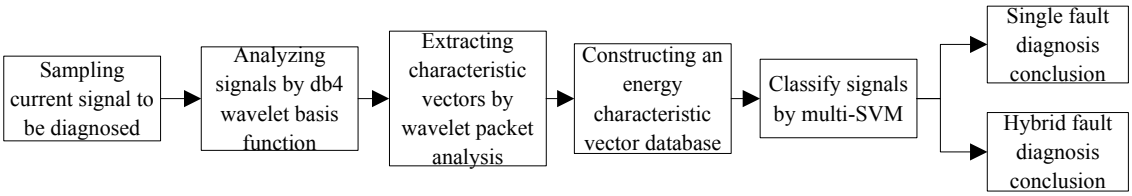

Figure 3. Fault diagnosis mechanism.

3 Results and discussion

3.1 Single fault diagnosis

Single fault diagnosis is the basis. When a fault occurs, output signal waveforms(n is the number of faults) of the (n+1)*100 plastic scintillation detector are simulated before and after the fault, and the eigenvectors are extracted by the wavelet packet algorithm according to variation characteristics of the waveforms. The eigenvectors of normalized fault signals and that of the normal signal are combined into a single fault diagnosis data sample set. 50% samples are selected for training the multi-SVM diagnostic model, and the remains are used for testing and performing fault diagnosis. The diagnostic accuracy is obtained through dividing the correct number of diagnosis groups by the total number of simulation samples. Table 2 to 5 presents the single fault diagnosis results.

Table 2. Aging fault diagnosis.

Scintillator luminous efficiency %	Correct sample number	Diagnostic accuracy %	Scintillator luminous efficiency %	Correct sample number	Diagnostic accuracy %
80	184	92	55	200	100
75	186	93	50	200	100
70	192	96	45	200	100
65	200	100	40	200	100
60	200	100	35	200	100

Table 3. Photomultiplier fault diagnosis.

Noise becomes n times the original	Diagnostic accuracy %	Noise becomes n times the original	Diagnostic accuracy %
n = 10	100	n = 13	100
n = 11	100	n = 14	100
n = 12	100	n = 15	100

According to the data in table 2 to 5, if a fault occurs, the diagnostic accuracy of plastic scintillators is above 92% due to the aging problem, and it will gradually increase as the luminous efficiency decreasing for the same reason. The diagnostic accuracy of the photomultiplier, RC, and radiation damage faults are 100%.

2020 JINST 15 T03001

Table 4. RC fault diagnosis.

RC becomes n times original	Diagnostic accuracy %	RC becomes n times original	Diagnostic accuracy %
$n = 1/4$	100	n = 4	100
$n = 1/5$	100	n = 5	100
$n = 1/6$	100	n = 6	100
$n = 1/7$	100	n = 7	100
$n = 1/8$	100	n = 8	100
n = 0	No output signal	n tends to infinity	100

Table 5. Radiation damage fault diagnosis.

Scintillator luminous efficiency %	Diagnostic accuracy %					
	10 times more noise	11 times more noise	12 times more noise	13 times more noise	14 times more noise	15 times more noise
35	100	100	100	100	100	100
45	100	100	100	100	100	100
55	100	100	100	100	100	100
65	100	100	100	100	100	100
75	100	100	100	100	100	100
85	100	100	100	100	100	100

3.2 Hybrid fault diagnosis

In real work conditions, plastic scintillation detectors may have a single fault, and sometimes multifaults may overlap each other. Consequently, analyzing the multifault mixing situation is necessary.Compared with single fault diagnosis, the hybrid one is more complex. As multiple faults superimposed on each other, the output signal waveforms are extracted by wavelet packet algorithm, then a multi-SVM model is established after the normalization to perform fault diagnosis. Firstly, this simulation experiment performed a mixed fault diagnosis of every two combining of four types. Figure 4 to 6 exhibits the various diagnostic results. Taking a combining of the scintillator aging fault and the photomultiplier fault for instance, the diagnosis results contains 10×6 groups (figure 4a), wherein an increase of noises caused by the photomultiplier fault has little effect on diagnostic accuracy, the luminous efficiency caused by the scintillator aging fault reduced, and it has impact on the diagnostic accuracy. That is, the diagnostic accuracy gradually increase as the scintillator aging problem gets worse. For the apparent features of faults, fault signals are easily distinguished from normal ones. When the luminous efficiency reduced to 70%, the diagnostic accuracy reaches 100%. However, the accuracy will fluctuate as a reduction of the luminous efficiency to the range of 65% to 50% due to the similarity between the normal waveform and the combined one, this combined one comes from the aging fault and the photomultiplier fault. Futhermore, the similarity may lead misclassfication. Figure 4b shows diagnostic results of a combination of the scintillator aging fault and the RC fault. Obviously, the diagnostic accuracy has

2020 JINST 15 T03001

a normal fluctuation when the luminous efficiency is in the range of 75% to 80%. If the RC value is less than 1, the diagnostic accuracy slightly reduced as the luminous efficiency attenuated from 65% to 50%. The reason is that fault waveform characteristics also have a certain similarity with the normal ones. Figure 5a shows diagnostic results of a combination of the scintillator aging fault and the radiation damage fault, and fluctuations of the diagnostic accuracy with similar to that of figure 4a. Figure 5b shows the diagnostic results of a combination of the RC fault and the radiation damage fault. Although the diagnostic accuracy fluctuates greatly and decreases sharply when the RC value reduced to 1/7 and which changes continuously, the final result will not be affected during the whole process. Figure 6a shows the diagnostic results of a combination of the photomultiplier fault and the RC fault. As portions of waveforms of RC circuits and the photomultiplier overlap on each other, they have a certain similarity with normal signals. If the RC value reduced to 1/8 and noises are 10 times of the original, the diagnostic accuracy has a drastic slide, and with noises multiplying, it rapidly rises to 100%. Figure 6b shows the diagnostic results of a combination of the photomultiplier fault and the radiation damage fault. It is more difficult for diagnosis procedure as the complexity of mixed signals from the radiation damage fault and the photomultiplier fault. As the radiation damage problem becomes more serious, the diagnostic accuracy fluctuates, and the average of that is still within a normal range. Secondly, this simulation experiment conducts hybrid diagnosis of three types of faults as well: the scintillator aging, the photomultiplier, and the RC circuit. Results of the three types are shown in figure 7, wherein the accuracy is represented in different colors. When the three kinds overlapped, an increase both in noises and the RC value which are caused by the photomultiplier fault and the RC fault respectively has little effect on the accuracy. Futhermore, it will gradually increase as the RC value becomes smaller which is from 1/4 to 1/8. The significant parameter which has a great influence on the diagnostic accuracy is the luminous efficiency. Generally, this influence is the same for the two combined faults. As the luminous efficiency decreases, the diagnostic accuracy gradually increases. However, there is a conversion at the range of 65% to 50% of the luminous efficiency. This conversion leads decreasing of the accuracy slightly. Results in figure 4 to 7 show that the average accuracy of hybrid fault diagnosis is lower than that of the single one. However, the minimum of average diagnostic accuracies with every combinations is still greater than 94%. This model can effectively diagnose faults in most cases.

Table 6 shows the accuracy of partial hybrid fault diagnosis. The data in table 6 show that the fault diagnosis method based on wavelet packet analysis and multi-SVM still has high diagnostic accuracy while performing hybrid fault diagnosis, and which can effectively diagnose scintillation detectors' faults.

4 Conclusions

For the various faults of scintillation detectors, this paper took the plastic scintillation detector as an example, discussed previous theories and experiments, proposed a fault detection model which is based on the wavelet packet analysis and the multi-SVM through extracting the characteristic vector of signals. This model identifies various faults through comparing the output signal waveform of the scintillation detector under normal operating conditions and under typical fault conditions. Numerous experiments show the model can quickly and accurately determine the fault types. Finally,

2020 JINST 15 T03001

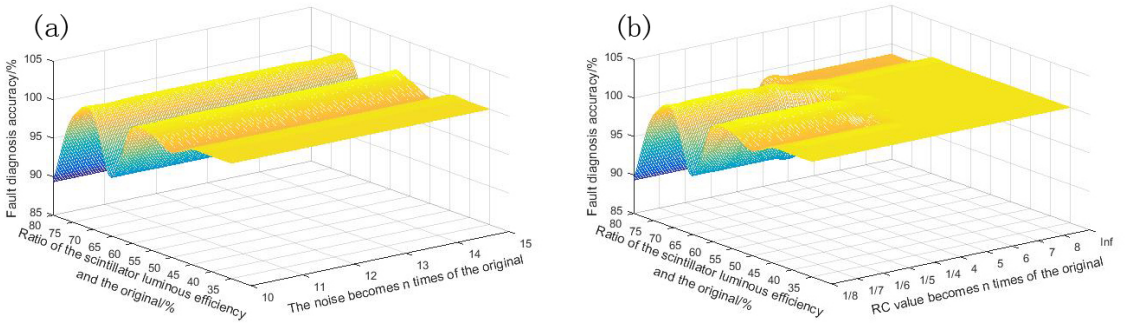

Figure 4. a Results of scintillator aging fault and photomultiplier fault diagnosis; b Results of scintillator aging fault and RC fault diagnosis.

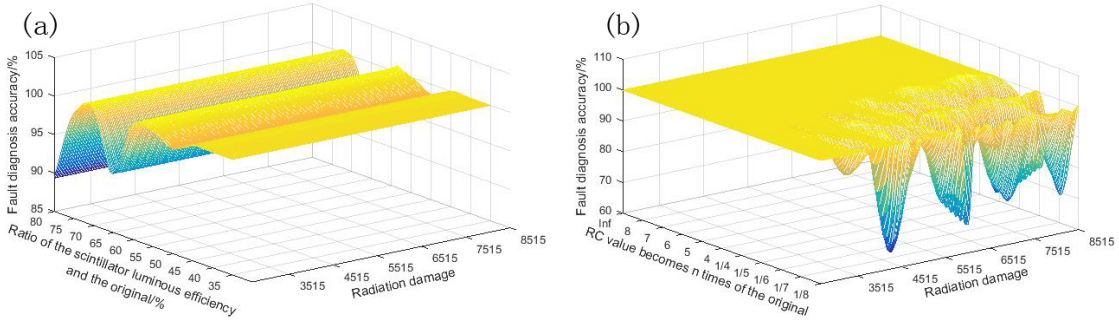

Figure 5. a Results of scintillator aging fault and radiation damage fault diagnosis; b Results of RC fault and radiation damage fault diagnosis.

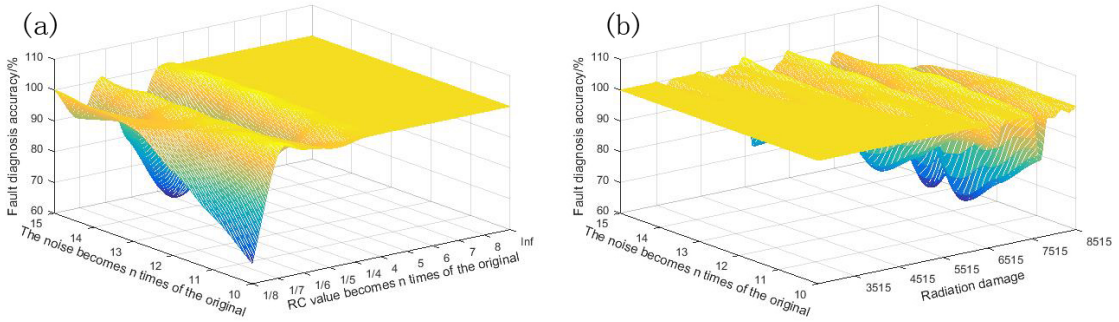

Figure 6. a Results of photomultiplier fault and RC fault diagnosis; b Results of photomultiplier fault and radiation damage fault diagnosis.

2020 JINST 15 T03001

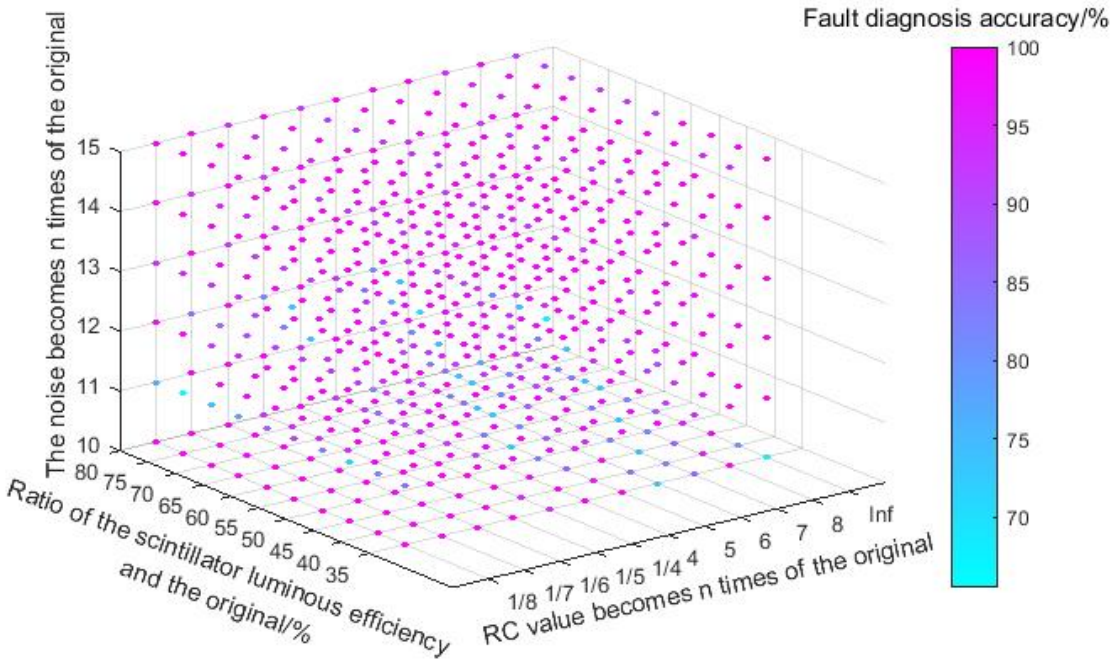

Figure 7. Results of scintillator aging fault, photomultiplier fault, and RC fault diagnosis.

Table 6. Part of the results of hybrid fault diagnosis.

Number	Fault type	Diagnosis result (group)	Diagnostic accuracy average %
1	Aging and photomultiplier	10×6	97.93
2	Aging and RC	10×11	98.92
3	Aging and radiation damage	10×36	97.93
4	Photomultiplier and RC	6×11	97
5	Photomultiplier and radiation damage	6×36	96.01
6	RC and radiation damage	11×36	98.34
7	Aging, photomultiplier, and RC	$10 \times 6 \times 11$	96.2
8	Aging, photomultiplier, and radiation damage	$10 \times 6 \times 36$	94.87

it is suitable for the intelligent fault diagnosis of various digital nuclear detection instruments. Also it has broad application prospects in the field of nuclear monitoring.

Acknowledgments

With sincere gratitude to all those who have helped me on this team. This work was supported by the National Natural Science Foundation of China (No. 11575081), the Natural Science Foundation of Hunan Province (No. 2018JJ2317), and the Hengyang Science and Technology Bureau Project of China (No. S2018G9031016324).

2020 JINST 15 T03001

References

[1] T.-H. Lin and S.-C. Wu, *Sensor fault detection, isolation and reconstruction in nuclear power plants*, *Annals Nucl. Energy* **126** (2019) 398.

[2] J. Ma and J. Jiang, *Applications of Fault Diagnosis in Nuclear Power Plants: An Introductory Survey*, *IFAC P. Volumes* **42** (2009) 1150.

[3] H.M. Hashemian, *Aging management of instrumentation & control sensors in nuclear power plants*, *Nucl. Eng. Des.* **240** (2010) 3781.

[4] H.M. Hashemian, *On-line monitoring applications in nuclear power plants*, *Prog. Nucl. Energy* **53** (2011) 167.

[5] J. Ma and J. Jiang, *Applications of fault detection and diagnosis methods in nuclear power plants: A review*, *Prog. Nucl. Energ.* **53** (2011) 255.

[6] J. Chen, H. Li, D. Sheng and W. Li, *A hybrid data-driven modeling method on sensor condition monitoring and fault diagnosis for power plants*, *Int. J. Elec. Power* **71** (2015) 274.

[7] E. Nasimi and H.A. Gabbar, *Signal de-noising methods for fault diagnosis and troubleshooting at CANDU® stations*, *Nucl. Eng. Des.* **280** (2014) 481.

[8] T. Alharbi, *Principal Component Analysis for pulse-shape discrimination of scintillation radiation detectors*, *Nucl. Instrum. Meth.* **A 806** (2016) 240.

[9] G.-M. Xian and B.-Q. Zeng, *An intelligent fault diagnosis method based on wavelet packer analysis and hybrid support vector machines*, *Expert Syst. Appl.* **36** (2009) 12131.

[10] H. Wang, M.-j. Peng, J. Wesley Hines, G.-y. Zheng, Y.-k. Liu and B.R. Upadhyaya, *A hybrid fault diagnosis methodology with support vector machine and improved particle swarm optimization for nuclear power plants*, *ISA Trans.* **95** (2019) 358.

[11] M. Fei, L. Ning, M. Huiyu, P. Yi, S. Haoyuan and Z. Jianyong, *On-line fault diagnosis model for locomotive traction inverter based on wavelet transform and support vector machine*, *Microelectron. Reliab.* **88–90** (2018) 1274.

[12] M. Tadeusiewicz and S. Hałgas, *A method for multiple soft fault diagnosis of linear analog circuits*, *Measurement* **131** (2019) 714.

[13] M. Hamel, M. Soumaré, H. Burešová and G.H.V. Bertrand, *Tuning the decay time of plastic scintillators*, *Dyes. Pigm.* **165** (2019) 112.

[14] A. Widodo and B.-S. Yang, *Support vector machine in machine condition monitoring and fault diagnosis*, *Mech. Syst. Signal Pr.* **21** (2007) 2560.

[15] R. Ortaç-Kabaoğlu, İ. Eksin, E. Yeşil and M. Güzelkaya, *Fault Detection and Diagnosis for Nonlinear Systems: A Support Vector Machine Approach*, *IFAC P. Volumes* **42** (2009) 355.

[16] J. Cui and Y. Wang, *A novel approach of analog circuit fault diagnosis using support vector machines classifier*, *Measurement* **44** (2011) 281.

[17] P.V.d. Kerkhof, J. Vanlaer, G. Gins and J.F.M. Van Impe, *Online batch fault diagnosis with Least Squares Support Vector Machines**, *IFAC P. Volumes* **45** (2012) 432.

[18] B.-S. Yang, W.-W. Hwang, D.-J. Kim and A. Chit Tan, *Condition classification of small reciprocating compressor for refrigerators using artificial neural networks and support vector machines*, *Mech. Syst. Signal Pr.* **19** (2005) 371.

[19] Q. Xu and Z. Li, *Recognition of wear mode using multi-variable synthesis approach based on wavelet packet and improved three-line method*, *Mech. Syst. Signal Pr.* **21** (2007) 3146.

2020 JINST 15 T03001